

1D Mathematical modelling of debris flow

Simulation numérique unidimensionnelle du charriage torrentiel

P. BRUFAU, P. GARCÍA-NAVARRO, *Mecánica de Fluidos. Centro Politécnico Superior. Universidad de Zaragoza. Spain.*

P. GHILARDI, L. NATALE, *Dipartimento di Ingegneria Idraulica e Ambientale. Università degli studi di Pavia. Italy.*

F. SAVI, *Dipartimento di Idraulica Trasporti e Strade. Università "La Sapienza" di Roma. Italy.*

ABSTRACT

Debris flow is modelled using the equations governing the dynamics of a liquid-solid mixture. An upwind finite volume scheme is applied to solve the resulting differential equations in one dimension. These equations have a structure similar to those of the monophasic water flow, differing from them by the presence of some terms characteristic of the bifasic nature of the mixture, such as granular bed erosion velocity, sediment concentration, bed shear stress, etc. The model and the system of equations to be solved are presented with the description of the implementation of the upwind scheme for the resulting hyperbolic conservation system. The numerical method is first order in both space and time. The treatment of the source terms is specified in detail and some comparison with laboratory experiments are presented.

RÉSUMÉ

Le charriage torrentiel est représenté par un système d'équations unidimensionnelles décrivant le comportement d'un mélange liquide-solide. La méthode numérique utilisée est une méthode aux volumes finis, utilisant une discrétisation de type 'upwind'. Les équations sont similaires dans leur forme à celles d'un écoulement à surface libre monophasique, mis à part la présence de quelques termes associés à la nature diphasique du mélange, tels que la vitesse d'érosion du lit granulaire, la concentration en sédiments, le cisaillement sur le fond, etc. Le système d'équations hyperboliques et la méthode numérique sont présentés. Cette méthode numérique est du premier ordre en espace et en temps. Le traitement des termes source fait l'objet d'une description détaillée et l'on présente des comparaisons avec des expériences en laboratoire.

1 Introduction

In mountain torrents, intense and localised storms may cause flash floods with important sediment transport. In steep torrents, the sediment discharge may increase so that the solid concentration often exceeds figures of 40-50%. This is the case of the debris flows that transport downstream huge volumes of sediments that are then deposited on the alluvial fans, often highly populated. These wide areas are periodically exposed to catastrophic events. To reduce the debris flow hazard, it is common to couple structural and non structural protections such as zoning of the risk prone areas and emergency plans. Protection plans require the description of scenarios that can be defined only by means of simulations with mathematical models.

In this paper a numerical model for unsteady debris flow is presented. The model will be applied to simulate different test conditions in channels with simple geometry. A one-dimensional scheme is proposed whilst a two-dimensional scheme for the more complex wave propagation on alluvial fans will be developed in future work.

Many authors have proposed mathematical models of debris flow based on the conservation of mass and momentum of the flow. Only some of them take into account the erosion/deposition process and the behaviour of different classes of sediment in the flow. The fluid is alternatively considered as a one-phase constant-density fluid or a two-phase variable-density mixture composed by granular material immersed in an interstitial fluid. This assumption strongly influences the choice of the rheological model: the typical situation of a debris flow stopping where the channel slope decreases may be simulated either with a constant density fluid or with a variable density mixture; but in the former case, the debris flow stops only if the rheological model

allows for a yield stress. On the other hand, in a variable density mixture, the sediments settle even though the interstitial fluid continues to flow downstream.

For the constant-density fluid, different rheological models were adopted in the past such as Bingham type model (Fracca-rollo 1995, Jan 1997, Jin and Fread 1997), Herschel-Bulkley model (Laigle and Coussot 1997) or quadratic shear stress model (O'Brien et al. 1993). Takahashi and Tsujimoto (1985), using a Bagnold rheological model in which the yield stress is not present, simulated the entire phenomenon considering separate mechanisms for deceleration, stopping and deposition stages. Rickenmann and Koch (1997) tested different rheological models varying from Bingham to Newtonian fluid (both in laminar and turbulent flow) and from dilatant to Voellmy fluid. A constant density fluid model cannot simulate the effects of sediments separation, needed to reproduce those real world events in which the coarser sediments settle in the upper part of the alluvial fan or near obstacles in the river bed.

Modelling the fluid as a two-phase mixture overcomes most of the limitations mentioned above, allowing for a wider choice of rheological models. Again, many alternatives can be found in the literature, for example: Bagnold's dilatant fluid hypothesis used by Takahashi (1991), Takahashi and Nakagawa (1994), Shieh et al. (1996); Chezy-type equation with constant value of the friction coefficient (Hirano et al. 1997, Armanini and Frac-carollo 1997); cohesive yield stress (Egashira et al. 1997), etc. Other rheological models were proposed for debris flow (see Chen 1988), and many of them can be easily used in numerical modelling. For a recent review see Hutter et al. 1996.

The change in the debris flow density can be modelled through the mass balance of both phases (solid and liquid), and the definition of the erosion/deposition rate as a function of sediments

Revision received July, 1999. Open for discussion till June 30, 2001.

concentration. Shieh et al. (1996) introduced an empirical non-equilibrium condition for concentration when deposition occurs, assuming that concentration varies from the equilibrium in the steeper reach to the equilibrium concentration in the flatter reach according to an exponential law; Armanini and Fraccarollo (1997) assumed the concentration equal to the equilibrium value. Egashira and Ashida (1987), Hirano et al. (1997), Honda and Egashira (1997), Mizuyama and Yazawa (1987) and Takahashi et al. (1987) developed 1D and 2D models which consider non-equilibrium conditions. The first three authors take only into account the coarse fraction, i.e. the interstitial fluid is nearly homogenous (water). The last two authors consider also variations of the concentration of the fine fraction in the interstitial fluid.

The erosion/deposition rate is controlled by the excess of the local instantaneous concentration over the equilibrium concentration. Egashira and Ashida (1987) and Honda and Egashira (1997) computed this rate by means of a simple relationship. Takahashi (1991) proposed semi-empirical expressions which differ from deposition to erosion and erosion produced in a saturated bed from that in an unsaturated bed is distinguished too. All these models ignore the spatial and temporal variations of debris flow density in the momentum balance equations.

Most of the above models are solved numerically with finite difference schemes. Takahashi and Tsujimoto (1985) used a centred differences scheme; Fraccarollo and Toro used an upwind scheme proposed by Toro (1996); Honda and Egashira (1997) proposed a technique based on backward differences, valid only for supercritical flow; other authors used Lagrangian schemes (see Savage and Hutter 1989, Iverson 1997, Rickenmann and Koch 1997).

In the present work granular and liquid phases are considered. The set of equations includes two mass conservation equations (one for the mixture and another for the solid phase) and a single momentum balance equation of the 1D flow. The spatial and temporal variation of debris flow density is included as a source term. The friction term is simulated according to Takahashi (1991). The system is completed with equations to estimate the erosion/deposition rate derived from the Egashira and Ashida (1987) or Takahashi (1991) relationships.

The set of equations is solved by means of an explicit finite volume technique based on first order Roe's scheme. The advection equation of the coarse solid fraction is solved in cascade at each time step after the momentum balance equation of the mixture has been integrated.

2 Governing equations

The two-phase mixture constituted by coarse sediment fraction and interstitial fluid is considered. The concentration of the finer solid fraction in the interstitial fluid is assumed to be negligible, so that the fluid acts as clean water. The same velocity for the coarser solid fraction and the interstitial fluid is assumed too, therefore a unique momentum equation is used. The flow of the solid-liquid mixture is described using a 1D depth averaged model that, apart from stating mass and momentum con-

servation of the debris, includes a solid phase mass conservation law and a bed evolution law. The set of four differential equations is presented in this section.

The equations describing the mixture and the coarse fraction mass balance and the mixture momentum along the main stream direction can be expressed in

$$\frac{\partial A}{\partial t} + \frac{\partial Q}{\partial x} = ib \quad (2.1)$$

$$\frac{\partial Q}{\partial t} + \frac{\partial \left(\frac{\beta Q^2}{A} + g \frac{A^2}{2b} \cos \theta \right)}{\partial x} = gA(S_o - S_f) \quad (2.2)$$

$$\frac{\partial(hc)}{\partial t} + \frac{\partial(hcu)}{\partial x} = ic_v \quad (2.3)$$

Mass and momentum balance equations for the mixture solid-liquid can be expressed in conservative form as (Chow 1959)

$$\frac{\partial \mathbf{U}}{\partial t} + \frac{\partial \mathbf{F}}{\partial x} = \mathbf{H} \quad (2.4)$$

with

$$\mathbf{U} = \begin{pmatrix} A \\ Q \end{pmatrix}, \mathbf{F} = \begin{pmatrix} Q \\ \beta \frac{Q^2}{A} + g \frac{A^2}{2b} \cos \theta \end{pmatrix}, \mathbf{H} = \begin{pmatrix} ib \\ gA(S_o - S_f) \end{pmatrix} \quad (2.4.1)$$

In (2.4) \mathbf{U} represents the vector of conservative variables, \mathbf{F} is the flux vector in the x direction, and \mathbf{H} is the source term. In addition, A is the flow cross section area, Q is the flow discharge, h is the depth of the debris flow, u is the mean velocity in a cross section, c is the dimensionless volumetric concentration of sediments in the mixture, c_v is a parameter related to the bed concentration of sediments to be defined later, b is the width of the channel, g is the acceleration due to gravity, i is the bed erosion/deposition velocity and β is the momentum correction coefficient that we will assume to take the value $\beta = 1$ from now on. The bed slope S_o is given by the bed inclination θ

$$S_o = \sin \theta = -\frac{\partial z}{\partial x} \quad (2.4.2)$$

where z is the bed level respect to an arbitrary horizontal reference. In the mathematical model we are presenting, the bed level may change in space and time so that definition of the bed evolution $z = z(x,t)$ is one of the objectives. These changes are represented as erosion and/or deposition phenomena. We have only modelled bottom movement in all the cases, avoiding the possible change of the channel vertical walls, as a preliminar work to check the capability of the model. On the other hand, rectangular cross sections have been assumed, although in future work arbitrary geometries for the cross sections with

their complete change in time and space will be considered as well as 2D problems.

For a detailed review of different equations describing the friction term, represented by S_f , see Chen (1988). In the present work, the Takahashi (1991) equations have been chosen according to the dilatant fluid hypothesis developed by Bagnold (1954). Two main different types of flow have been distinguished:

- For low concentrations of the coarse fraction in water ($c \leq 0.2$), friction is modelled by a typical open channel law and the flow is classified as *immature* debris flow. The Manning's equation for friction used in open channel free surface flows (Chow 1959), is replaced by

$$S_f = \frac{d^2 u^2}{0.49 g h^2 R_h} \quad (2.5)$$

In this law, d is the mean effective diameter of the sediment particles and R_h is the hydraulic radius $R_h = A/P$ where P is the wetted perimeter. For rectangular channels $P = b + 2h$.

- More complicated dependences appear when the concentration of solid is important ($c \geq 0.2$). In that case the flow is classified as *stony* debris flow and the law suggested by Takahashi (1991) is

$$S_f = \frac{u^2}{\left(\frac{2}{5d\lambda}h\right)^2 \frac{1}{a_B \sin\alpha} \left[c + (1-c) \frac{\rho_l}{\rho_s} \right] g R_h} \quad (2.6)$$

An explicit dependence on the concentration is shown in (2.6). Moreover, the quantity λ , linear concentration, depends on the granulometry of the solids in the form

$$\lambda = \left[\left(\frac{c^*}{c} \right)^{\frac{1}{3}} - 1 \right]^{-1} \quad (2.7)$$

where c^* is the coarse fraction concentration in the static debris bed, a_B is an empirical constant (Bagnold (1954) assumed $a_B = 0.042$), α is the dynamic internal angle of friction, and ρ_s , ρ_l are the sediment and water density respectively.

These resistance equations were validated through experiments in flumes with almost smooth and fixed walls. In presence of a static granular bed, the roughness is significantly higher. Takahashi (1991) fitted his experimental data in flumes with almost smooth and fixed walls using for a_B the value given by Bagnold $a_B = 0.042$. In presence of an erodible granular bed, he found significantly higher resistance so the value of a_B was increased to 0.35-0.5.

When the sediment concentration is high, the resistance is mainly caused by the dispersive stress and the roughness of the bed does not influence the resistance (Scotton and Armanini 1992). For low values of the sediment concentration or $\frac{h}{d} > 30$, the energy dissipation is mainly due to the turbulence in the interstitial fluid and the influence of the wall roughness

becomes important. In such case, Takahashi (1991) suggests the use of Manning's equation or similar resistance laws.

It is worth noting that density is not present in these equations as a variable. The underlying assumption is that, being different from water density, there is a uniform and constant debris density. This will be reconsidered at the end of this section.

The mass balance equation in (2.1) expresses actually volume conservation of the mixture. Therefore, the bed erosion/deposition velocity i appears as a source term. The dependence of this quantity with the basic set of dependent variables has to be modelled. In this work two models have been chosen; a simple one proposed by Egashira and Ashida (1987) in the form

$$i = K u \tan(\theta - \theta_e) \quad (2.8)$$

involving the difference between the bed slope (θ) and the equilibrium angle (θ_e). The empirical coefficient K is assumed equal to 1 by Egashira and Ashida.

The equilibrium angle is a relevant parameter that depends mainly on the concentration of the mixture and on the density ratio $s = \rho_s/\rho_l$ between solid and water. When the inclination of the channel bed has reached the equilibrium angle, no erosion or deposition occurs and a steady bottom state can be defined. This variable will determine the test cases to check the scheme.

$$\theta_e = \arctan\left(\tan\phi \frac{c(s-1)}{c(s-1)+1} \right) \quad (2.9)$$

ϕ is the static internal friction angle and c is the sediment volumetric concentration. A positive value of i means that erosion takes place, otherwise deposition occurs until equilibrium is reached.

In case a debris front advances over an adverse slope,

$$\frac{\partial z}{\partial x} \geq 0 \Rightarrow S_0 \leq 0 \Rightarrow \theta \leq 0 \Rightarrow i \leq 0 \quad (2.10)$$

and equation (2.8) will always tend to deposition even when erosion should occur. In order to overcome this difficulty a modification of the equation is proposed in this work

$$i = K u \tan(\theta_f - \theta_e) \quad (2.11)$$

where

$$\theta_f = \arctan\left(\frac{S_f}{\cos\theta} \right) \quad (2.12)$$

being S_f the slope of the energy line. When there is a uniform flow, $\theta_f = \theta$, and if $K = 1$, equation (2.11) becomes equal to the original expression proposed by Egashira and Ashida (2.8). Although (2.11) is introduced as an alternative expression of (2.8) for adverse slope reaches, it should be noted that (2.11) is

valid also for the entire channel independently of the sign of the bottom slope.

The original model from Egashira and Ashida (2.8) is based on the assumption of normal flow so driven by the bed slope. Instead, (2.11) implies that the erosion/deposition is forced by the energy line slope and is associated to a slower process of erosion/deposition in general, shown in Fig. 2.

Modifying the Takahashi's equations (1991), Ghilardi and Natale (1998) derived the following expressions for the erosion/deposition rate. Takahashi (1991) distinguishes when deposition or erosion take place; if erosion occurs ($c > c'_{eq}$) in presence of a saturated bed, i is calculated in the form

$$i = \delta_e \frac{c'_{eq} - c}{c^* - c_{eq}} \cdot \frac{\tan \phi - \tan \theta_f h u}{\tan \phi - \tan \theta d} \quad (2.13)$$

where c'_{eq} is the equilibrium concentration for non-uniform flow

$$c'_{eq} = \frac{\tan \theta_f}{(s-1)(\tan \phi - \tan \theta_f)} \quad (2.14)$$

and c_{eq} represents the equilibrium concentration for uniform flow

$$c_{eq} = \frac{\tan \theta}{(s-1)(\tan \phi - \tan \theta)} \quad (2.15)$$

being δ_e an empirical constant adjusted with experimental measurements. Takahashi proposed $\delta_e = 7 \cdot 10^{-4}$ for erosion, and in case equilibrium state is predicted, it seems to agree with physical phenomena. In order to fit the experimental results given by Gregoretti (1996), the value of δ_e has been increased one order of magnitude, $\delta_e = 7 \cdot 10^{-3}$.

Otherwise, when deposition occurs, the model adopted for the deposition velocity is

$$i = \delta_d \frac{c'_{eq} - c}{c^*} u \quad (2.16)$$

with $0.05 \leq \delta_d \leq 1$, an empirical constant for deposition as well as δ_e for erosion. In the tests presented, the value chosen is $\delta_d = 0.05$.

For physical reasons, $c_{eq}, c'_{eq} \leq m c^*$, being the value of the empirical constant $m = 0.9$ (Takahashi 1991) or 0.95 (Yazawa and Mizuyama 1987), derived from experimental observations. Since in real world cases the maximum values of c_{eq} and c'_{eq} are often reached, the value of m strongly influences the results.

The equation for the sediment mass conservation, (2.3), is again established as a volume balance and repeated here for completeness

$$\frac{\partial(hc)}{\partial t} + \frac{\partial(hcu)}{\partial x} = i c_v \quad (2.17)$$

c_v is a parameter of the model related to the concentration of sediments in the bed layer.

$$c_v = \begin{cases} \max(c, c_D^*) & i \leq 0 \\ c^* & i > 0 \end{cases} \quad (2.18)$$

where c_D^* is the volumetric sediment concentration on a static bed just after deposition.

Finally, when the cross section of the channel is rectangular with fixed walls and loose bottom, the movement of the bed due to erosion or deposition processes that take place in presence of a given sediment concentration is represented by the following equation

$$\frac{\partial z}{\partial t} \cos \theta + i = 0 \quad (2.19)$$

The complete set of partial differential equations to solve is

$$\frac{\partial A}{\partial t} + \frac{\partial Q}{\partial x} = i b \quad (2.20)$$

$$\frac{\partial Q}{\partial t} + \frac{\partial \left(\frac{Q^2}{A} + g \frac{A^2}{2b} \cos \theta \right)}{\partial x} = g A (S_0 - S_f) \quad (2.21)$$

$$\frac{\partial(hc)}{\partial t} + \frac{\partial(hcu)}{\partial x} = i c_v \quad (2.22)$$

$$\frac{\partial z}{\partial t} \cos \theta + i = 0 \quad (2.23)$$

for the variables A, Q, z, c . They form a closed set if (2.5) or (2.6), (2.11) or (2.13) and (2.16) are used.

Another form of the equations has been adopted to permit density changes in time and space in a suitable and simple way. In this case equation (2.2) has been replaced by

$$\frac{\partial(\rho Q)}{\partial t} + \frac{\partial \left(\rho \frac{Q^2}{A} + g \rho \frac{A^2}{2b} \cos \theta \right)}{\partial x} = \rho g A (S_0 - S_f) \quad (2.24)$$

The debris density ρ can be expressed in terms of the concentration c , the solid density ρ_s and the liquid density ρ_l ,

$$\rho = \rho_s c + \rho_l (1 - c) \quad (2.25)$$

The rest of equations remain the same. With algebraic operations, isolating the terms that contain ρ and using the continuity equation we arrive to

$$\frac{\partial Q}{\partial t} + \frac{\partial \left(\frac{Q^2}{A} + g \frac{A^2}{2b} \cos \theta \right)}{\partial x} = gA(S_0 - S_f) - \left[\frac{bui}{\rho} (\rho_v - \rho) + \frac{gA^2}{\rho 2b} \cos \theta \frac{\partial \rho}{\partial x} \right] \quad (2.26)$$

where

$$\rho_v = \begin{cases} \rho_D^* & i \leq 0 \\ \rho^* & i > 0 \end{cases} \quad (2.27)$$

ρ^* is the density of static bed and ρ_D^* the density of static bed just after deposition. The new term in the right hand side containing density variations has been treated as a source term and has been discretized explicitly like the other source terms.

Comparisons of these two models for the momentum equation have been carried out in all the numerical test cases without showing any appreciable difference in the results. The debris density variations are not strong enough to change the value of the variables. This confirms the hypothesis followed by several authors (Mizuyama and Yazawa 1987, Nakagawa and Takahashi 1997), who ignore the effects of the spatial and temporal variations of density in the momentum balance equation.

3 Numerical model

The domain where the variables are going to be calculated is divided in a temporal-spatial computational mesh. Each point is represented by the pair (x_j, t^n) , where x_j represents the position in the space $j = 1, 2, \dots, JMAX$ and t^n the time level $n = 1, 2, \dots, N$.

Upwind schemes are based on discretizations depending on the form of the equation and on the solution itself, taking into account the physical influence domain of every point in the mesh. They have proved well suited for the numerical solution of conservation laws.

In an explicit form, the first order upwind scheme for equation (2.4) can be written as:

$$\mathbf{U}_j^{n+1} = \mathbf{U}_j^n - \frac{\Delta t}{\Delta x} (\mathbf{F}_{j+\frac{1}{2}}^* - \mathbf{F}_{j-\frac{1}{2}}^*) + \Delta t \cdot \mathbf{H}_j^n \quad (3.1)$$

This cell-wise formulation is based on a balance over cell j with $\Delta x = x_{j+\frac{1}{2}} - x_{j-\frac{1}{2}}$ and $x_{j+\frac{1}{2}} = \frac{1}{2}(x_j + x_{j+1})$. In this work, a uniform mesh has been chosen in space.

$F_{j+\frac{1}{2}}^*$ is the numerical flux defined by

$$\mathbf{F}_{j+\frac{1}{2}}^* = \frac{1}{2} \left[\mathbf{F}_{j+1} + \mathbf{F}_j - \left| \tilde{\mathbf{A}}_{j+\frac{1}{2}} \right| \cdot (\mathbf{U}_{j+1} - \mathbf{U}_j) \right] \quad (3.2)$$

and is based on Roe's approximated Jacobian of the flux (Roe 1981).

The construction of the upwind scheme goes through a local linearization of the system of equations

$$\frac{\partial \mathbf{U}}{\partial t} + \mathbf{A} \frac{\partial \mathbf{U}}{\partial x} = \mathbf{H} \quad (3.3)$$

with

$$\mathbf{A} = \frac{\partial \mathbf{F}}{\partial \mathbf{U}} = \begin{pmatrix} 0 & 1 \\ v^2 - u^2 & 2u \end{pmatrix} \quad (3.4)$$

$v = \sqrt{gh \cos \theta}$ is the celerity of the linear surface waves. A new, approximated matrix $\mathbf{A}_{j+(1/2)}$ is defined with the following properties

- 1) $\tilde{\mathbf{A}}_{j+\frac{1}{2}} = \tilde{\mathbf{A}}_{j+\frac{1}{2}}(\mathbf{U}_{j+1}, \mathbf{U}_j)$,
- 2) $\mathbf{F}_{j+1} - \mathbf{F}_j = \tilde{\mathbf{A}}_{j+\frac{1}{2}} \cdot (\mathbf{U}_{j+1} - \mathbf{U}_j)$,
- 3) $\tilde{\mathbf{A}}_{j+1/2}$ has real and distinct eigenvalues and a complete set of eigenvectors and
- 4) $\tilde{\mathbf{A}}_{j+1/2}(\mathbf{U}_j, \mathbf{U}_j) = \mathbf{A}(\mathbf{U}_j)$.

Roe (1981) proposed $\tilde{\mathbf{A}}_{j+1/2}$ for the Jacobian matrix of the exact flux evaluated in an average state $\mathbf{A}(\tilde{\mathbf{U}}_{j+1/2})$. Therefore, the problem is moved to the computation of this averaged state, which is obtained imposing property (2).

Since the eigenvalues and eigenvectors of the \mathbf{A} matrix are:

$$a^{1,2} = u \pm v \quad (3.5)$$

$$\tilde{e}^{1,2} = \begin{pmatrix} 1 \\ a^{1,2} \end{pmatrix} \quad (3.6)$$

Average values $\tilde{u}_{j+1/2}$ and $\tilde{v}_{j+1/2}$ are used to define similar eigenvalues and eigenvectors of the approximated matrix $\mathbf{A}(\tilde{\mathbf{U}}_{j+1/2})$:

$$\tilde{a}_{j+\frac{1}{2}}^{1,2} = \tilde{u}_{j+\frac{1}{2}} \pm \tilde{v}_{j+\frac{1}{2}} \quad (3.7)$$

$$\tilde{e}_{j+\frac{1}{2}}^{1,2} = \begin{pmatrix} 1 \\ \tilde{a}_{j+\frac{1}{2}}^{1,2} \end{pmatrix} \quad (3.8)$$

From property (2) and the condition

$\mathbf{U}_{j+1} - \mathbf{U}_j = \sum_{k=1,2} \alpha_k \tilde{e}_{j+\frac{1}{2}}^k$ is easy to deduce that

(Alcrudo and García-Navarro 1992)

$$\tilde{u}_{j+\frac{1}{2}} = \frac{\sqrt{h_{j+1}} u_{j+1} + \sqrt{h_j} u_j}{\sqrt{h_{j+1}} + \sqrt{h_j}} \quad (3.9)$$

$$\tilde{v}_{j+\frac{1}{2}} = \sqrt{g \frac{h_{j+1} \cos \theta_{j+1} + h_j \cos \theta_j}{2}} \quad (3.10)$$

$$\alpha_{j+\frac{1}{2}}^{1,2} = \frac{h_{j+1} - h_j}{2} \pm \frac{1}{2\tilde{v}_{j+\frac{1}{2}}} \left[(hu)_{j+1} - (hu)_j - \tilde{u}_{j+\frac{1}{2}}(h_{j+1} - h_j) \right] \quad (3.11)$$

Then, the numerical flux corresponding to the first order upwind scheme given in (3.2) can be written as

$$\mathbf{F}_{j+\frac{1}{2}}^* = \frac{1}{2} \left[\mathbf{F}_{j+1} + \mathbf{F}_j - \sum_{k=1,2} |\tilde{a}_{j+\frac{1}{2}}^k| \alpha_{j+\frac{1}{2}}^k \tilde{\mathbf{e}}_{j+\frac{1}{2}}^k \right] \quad (3.12)$$

In order to avoid the problem of numerical solutions with non-physical discontinuities (zero eigenvalues), incompatible with the entropy principle, Harten and Hyman (1983) proposed the redefinition of the absolute value of the eigenvalues of $\tilde{A}_{j+\frac{1}{2}}$. It is necessary on this purpose to define the quantity $\epsilon_{j+\frac{1}{2}}^k$

$$\epsilon_{j+\frac{1}{2}}^k = \max \left[0, \left(\tilde{a}_{j+\frac{1}{2}}^k - a_j^k \right), \left(a_{j+1}^k - \tilde{a}_{j+\frac{1}{2}}^k \right) \right] \quad k = 1, 2 \quad (3.13)$$

The new absolute values of the eigenvalues are defined as

$$\Psi_{j+\frac{1}{2}}^k = \begin{cases} |\tilde{a}_{j+\frac{1}{2}}^k| & \text{if } |\tilde{a}_{j+\frac{1}{2}}^k| \geq \epsilon_{j+\frac{1}{2}}^k \\ \epsilon_{j+\frac{1}{2}}^k & \text{if } |\tilde{a}_{j+\frac{1}{2}}^k| < \epsilon_{j+\frac{1}{2}}^k \end{cases} \quad (3.14)$$

The source terms have been discretized pointwise in space and explicitly in time, except the friction term that has been treated in an implicit way to improve numerical stability. At the beginning of this work great difficulties with source terms arose. The flow advance over an initially dry bed and huge friction terms produced oscillations and finally the explosion of the code. This problem was solved evaluating the discharge in friction term at time level $n+1$.

For example, in equation (2.5) the new friction term considered is

$$S_f = \frac{d^2 Q^2}{0.49 g h^4 R_h} \cong \left(\frac{d^2}{0.49 g h^4 R_h} \right)^n (Q^2)^{n+1} \quad (3.15)$$

In this case, the discretized equation (3.1) for the momentum equation (2.2), is replaced by the following second order equation

$$D_j^n (Q^2)_j^{n+1} + Q_j^{n+1} + E_j^n = 0 \quad (3.16)$$

where

$$D = \Delta t g A \frac{S_f}{Q^2} \quad (3.17)$$

and

$$E = - \left[Q_j - \frac{\Delta t}{\Delta x} \left(\mathbf{F}_{j+\frac{1}{2}}^* - \mathbf{F}_{j-\frac{1}{2}}^* \right) + \Delta t g A S_0 \right] \quad (3.18)$$

Equation (3.16) is solved as an ordinary second order equation evaluating before the sign that the discharge variable should have.

$$Q_j^{n+1} = \text{sign}(Q_j^{n+1}) \frac{-1 + \sqrt{1 - 4DE}}{2D} \quad (3.19)$$

where

$$\text{sign}(Q_j^{n+1}) = \text{sign} \left(Q_j - \frac{\Delta t}{\Delta x} \left(\mathbf{F}_{j+\frac{1}{2}}^* - \mathbf{F}_{j-\frac{1}{2}}^* \right) + \Delta t g A S_0 \right) \quad (3.19.1)$$

because physically the friction term is not capable of changing the sign of the discharge.

Equation (2.3) is discretized in the same form as (2.4), although it is a scalar non-linear equation instead of a non-linear system of equations. The equation can be written in the same form as (2.4)

$$\frac{\partial w}{\partial t} + \frac{\partial f}{\partial x} = s \quad (3.20)$$

where

$$\begin{aligned} w &= hc \\ f &= huc \\ s &= ic_v \end{aligned} \quad (3.21)$$

Using the conservative formulation, an upwind scheme can be applied in the form we have described before being the updating at node j performed as

$$w_j^{n+1} = w_j^n - \frac{\Delta t}{\Delta x} \left(f_{j+\frac{1}{2}}^* - f_{j-\frac{1}{2}}^* \right) + \Delta t \cdot s_j^n \quad (3.22)$$

Now,

$$f_{j+\frac{1}{2}}^* = \frac{1}{2} \left[f_j + f_{j+1} - |\tilde{a}_{j+\frac{1}{2}}| (w_{j+1} - w_j) \right] \quad (3.23)$$

$$\text{and } a = \frac{df}{dw} = u, \tilde{a} = \frac{1}{2} (u + u_{j+1})$$

Finally, the discretization of equation (2.19) has been done explicitly, and the unknown z is calculated in the form

$$z_j^{n+1} = z_j^n - \frac{\Delta t \cdot l_j^n}{\cos \theta} \quad (3.24)$$

Forward Euler time integration has been used and the stability criterion adopted is

$$\Delta t = CFL \frac{\Delta x}{\max(|u| + v)} \quad (3.25)$$

CFL is the Courant number. It is worth noting that the condition $CFL \leq 1$ is not sufficient in this case since the region of stability detected is restricted to time steps requiring $CFL \leq 0.25$. This is due to the significant source terms in the equations.

4 Results

A selection of test cases were run to verify the convergence of the computed profiles to a final steady state and to prove the capability of the algorithm to simulate complex situations with transitions from supercritical to subcritical conditions and flows on adverse slopes. All the numerical experiments are carried out by releasing abruptly a constant discharge debris flow on a saturated bed without overland flow.

The numerical tests refer to debris flow on bed slopes evolving to equilibrium in a 30m long flume. The characteristics of coarse sediments and interstitial fluid $d, \phi, \alpha, \delta, c^*$ are defined as well as the values of the empirical parameters; thus, for an assigned value of θ_e and a constant inflow discharge Q , the corresponding values for uniform flow depth and concentration can be computed by means of equations (2.9) and (2.6). These values are imposed at the upstream section of the channel. It is verified that the simulated debris flow is stony.

At the downstream section it is assumed that debris flow quits the flume. The evolution of the debris flow is very rapid in all tested cases. Parameters used in the simulations are: $\Delta x = 1m$ as spatial interval, Courant number $CFL = 0.2$ for stability conditions, $b = 1m$ width of the flume, water density as 1000 Kg/m^3 $\phi = \alpha = 36^\circ$, $a_B = 0.04$ and $c^* = c_D^* = 0.7$, $K = 1$, $m = 0.9$. The computational time in all the tests has been a few minutes on standard PC and Unix workstations.

Both, Egashira and Ashida and Takahashi relations for the estimation of the erosion/deposition rate were used; obviously the results are the same at the final equilibrium state, but different transient conditions arise. In all the tested cases, we found that the variability of the mixture density in the momentum equation can be neglected because it does not affect the computed values of the variables. Therefore, the numerical experiments confirm the rightness of the assumptions of several authors (Mizuyama and Yazawa 1987, Nakagawa and Takahashi 1997) who ignored the effects of spatial and temporal variations of density in the momentum equation.

Erosion or deposition on uniform slope

The first numerical simulations presented here, consider a debris current flowing in a $L = 30m$ long reach with uniform initial bed slopes of $\theta = 2\theta_e$ and $\theta = \frac{\theta_e}{2}$, respectively. The values of $\theta_e = 12.5^\circ$, $h_o = 0.043m$, $u_o = 0.972m/s$ and $c_o = c_{eq}$ are used. At the upstream section of the flume the Froude number is 1.5. Other parameters used in these test cases are $\rho_s = 2000 \text{ Kg/m}^3$ as sediment density and $d = 0.005m$ mean diameter of sediment particles.

Fig. 1 shows the evolution of a channel bed profile computed for the erosion and deposition tests at the initial, intermediate and final positions at different times using the bottom slope in equations (2.8) (Egashira and Ashida model using the bottom slope). A difference in the time scale of the two processes can be noticed. It is justified by the initial values of the bed slope and the dependence of the erosion/deposition velocity on this angle. In Fig. 2a and 2b, profiles computed with this alternative and computed with the friction slope (2.11) are compared at $t = 8s$, after the erosion started. The dashed line represents the bottom and the straight line the free surface of the debris flow. Similar profiles can be obtained with equations (2.13) and (2.16) (Takahashi modified model). One may notice how the use of the two alternatives changes dramatically the results of the simulation in the transient: erosion/deposition process forced by the bed slope is faster than forced by the energy line slope. For more details, see section 2.

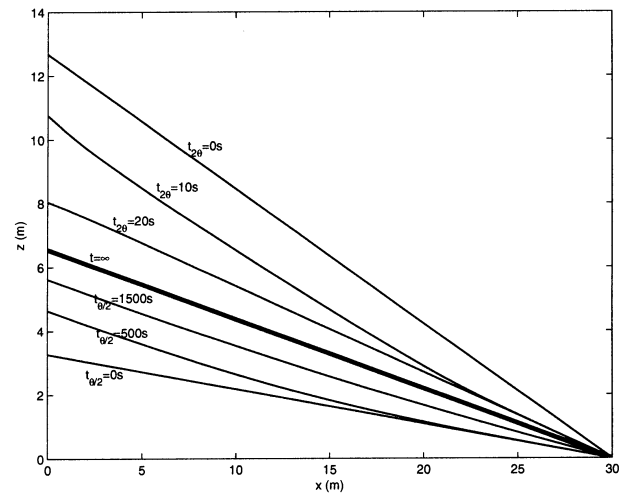


Fig. 1. Initial, intermediate and final states of the bed level.

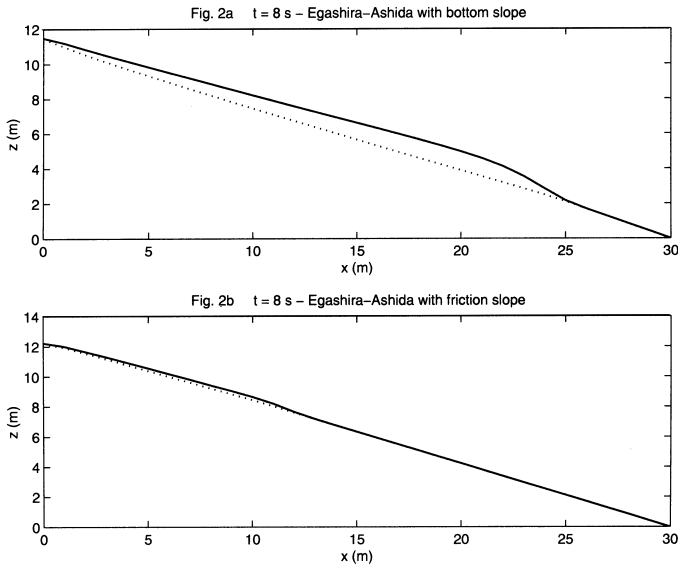


Fig. 2. Comparison of the numerical results using the bottom slope or the friction angle for the erosion/deposition rate. Bottom represented by the dashed line and debris free surface by the continuous one.

Erosion and deposition in a channel with two different slopes

This second test case consists of the same reach with two different initial bed slopes of 23° in the first $15m$ and 3° in the rest, $\theta_e = 8^\circ$. Debris flow is introduced upstream, with $h_o = 0.043m$, $u_o = 3.086m/s$, $c_o = 0.44$, Froude number = 2.5. It is assumed either non-erodible and erodible bed in the upper reach. From these initial conditions the debris moves and erosion/deposition processes take place until the equilibrium is reached and uniform flow achieved. After that moment no erosion or deposition occur.

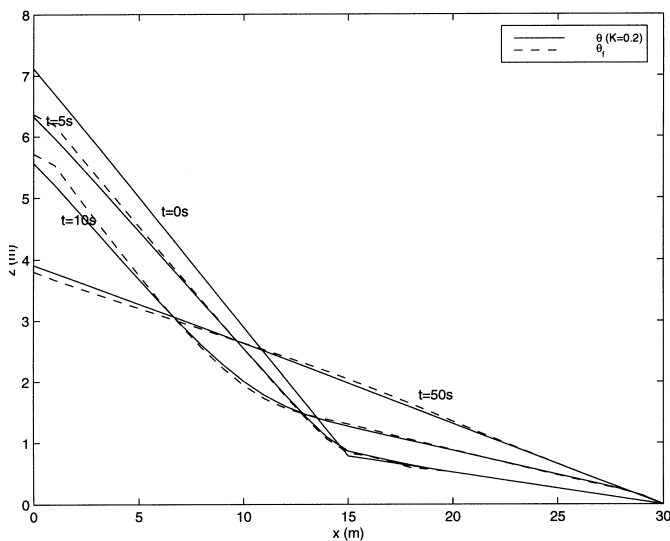


Fig. 3. Bottom slope evolution computed using Egashira ($K=0.2$) and the friction slope ($K=1$).

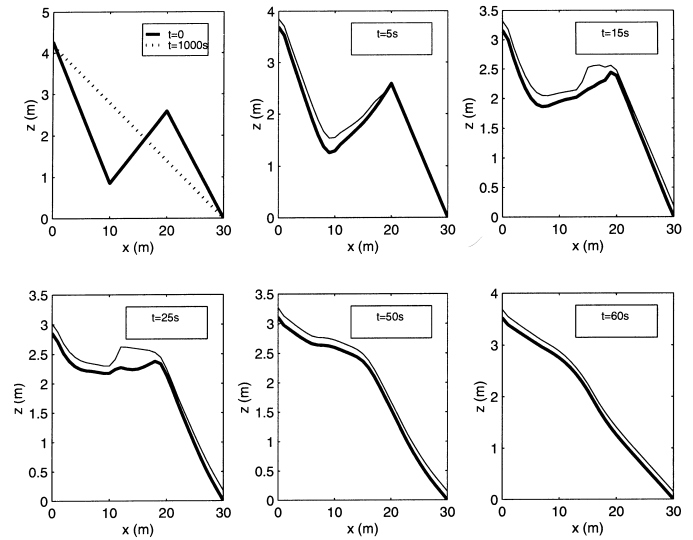


Fig. 4. Bed level time evolution at different time steps: $t = 0, 5, 15, 25, 50, 60$ and $1000s$. The thick line represents the bed level and the thin one the debris free surface.

Other parameters used in the modelling are: $\rho_s = 1600Kg/m^3$ as sediment density and $d = 0.001m$ mean diameter of sediment particles. The simulations are carried out with Egashira's model using the bottom slope and the energy line slope.

Fig. 3 presents the bottom elevation during the transient till equilibrium is achieved in case of erodible bed in the upper reach.

Adverse slope

In channels with an adverse slope the use of the bottom slope in the erosion/deposition equation does not allow for erosion on the counterslope: this fact causes incongruities in the simulation, that in some cases can be overcome only by means of numerical expedients. Three different initial bed slopes of 25° in the first $10m$, -15° from $10m$ till $20m$, and 25° in the rest are initially set up in this case. Upstream, debris flow conditions introduced are $h_o = 0.162m$, $u_o = 3.086m/s$ and $c_o = 0.4$, Froude number = 2.5, which are the equilibrium conditions for a 8° bed slope.

Parameters used in the modelling are: $\rho_s = 1600Kg/m^3$ as sediment density and $d = 0.01m$ mean diameter of sediment particles. The solution to the problem of the debris advancing over an adverse slope, explained in detail in section 2 (equation 2.11), is completely justified with this and the following test.

Fig. 4 presents the bed level evolution at different time steps till the final equilibrium state after $t = 1500s$ is achieved. It may be noticed that:

- an abrupt transition from supercritical to subcritical flow occurs in the reach with negative bottom slope,
- at the toe of the counterslope, the bottom is initially eroded and
- regressive erosion lowers the top of the counterslope.

The model does not include a special treatment for simulating erosion or deposition where surge happens. At the end, the equilibrium slope is reached.

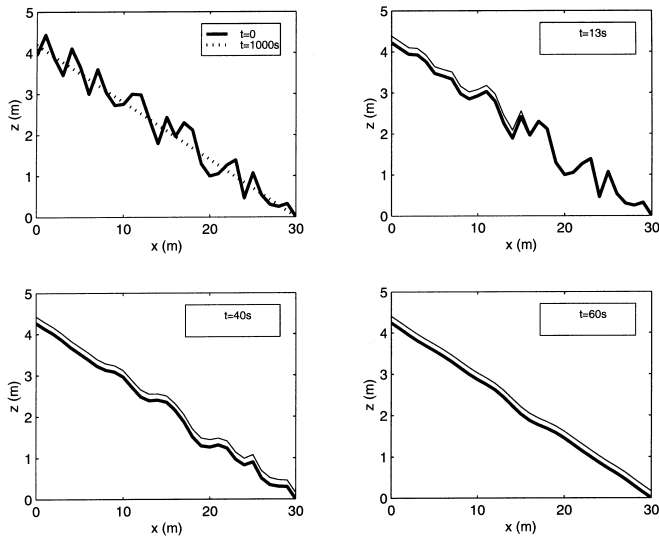


Fig. 5. Bed level time evolution at different time steps: $t = 0, 13, 40, 60$ and $1000s$. The thick line represents the bed level and the thin one the debris free surface.

Irregular bed

Different bed slopes are assumed along a reach. The evolution of a debris flow over an initially irregular dry bed level, reaching satisfactorily the equilibrium state, is checked. Debris flow upstream is $h_o = 0.162m$, $u_o = 3.086m/s$, $c_o = 0.4$, Froude number=2.45, which are the equilibrium conditions for a 8° bed slope.

Parameters used in the modelling are: $\rho_s = 1600Kg/m^3$ as sediment density and $d = 0.01m$ mean diameter of sediment particles.

Fig. 5 presents the bed evolution from the initial to the final position at different times: $t = 0s$, $t = 13s$, $t = 40s$, $t = 60s$ and $t = 1000s$. In this test, the erosion/deposition rate was computed with the Egashira model using (2.11).

Experimental test

To evaluate the capability of the model to reproduce real world phenomena, the experimental results obtained by Gregoretti (1996) are simulated. Gregoretti's experimental data are compared to numerical results obtained using the modified Egashira expression (2.11) where friction slope is introduced. In this test, debris flow is originated from the progressive erosion of a steep, saturated slope, in a rather short flume, $2.1m$ long in horizontal, with initial angle of 21° , formed by granular material contained between two vertical side walls $0.15m$ wide.

Three different homogenous grain sizes ($2, 7, 22mm$) and three different mixtures of the above grains were used. The values of the ratio h/d vary from 3 to 20. A narrow vertical tank communicating to the slope through a wire mesh feeds clean water. To simulate the delivering system, the model assumes that the

upstream section of the slope is a control section. Measured data are flow depth at the end of the reach and total outflow discharge. Changes in bed slope and sediment concentration were evaluated computing input and output discharges and eroded/deposited volumes. For details on the experimental setup see Gregoretti (1996) and Di Silvio and Gregoretti (1997).

Some comparisons are presented here: for stony debris flow in Fig. 6 and 7, for debris flow changing from stony to immature in Fig. 8 and 9 and for immature debris flow in Fig. 10 and 11.

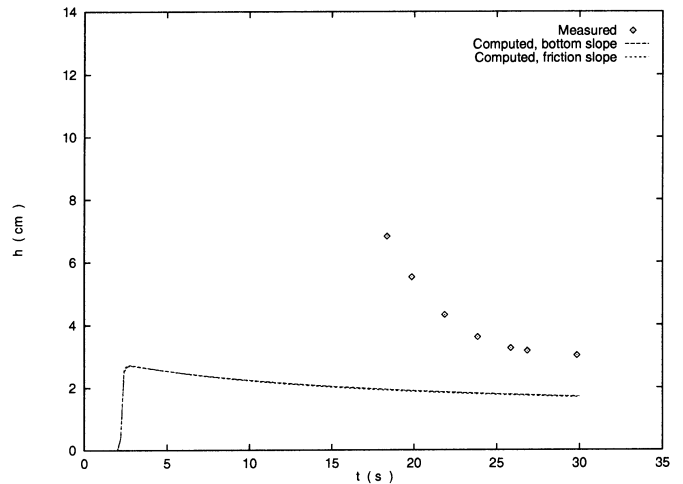


Fig. 6. Time evolution of the depth of debris at the end of the reach. Stony debris flow.

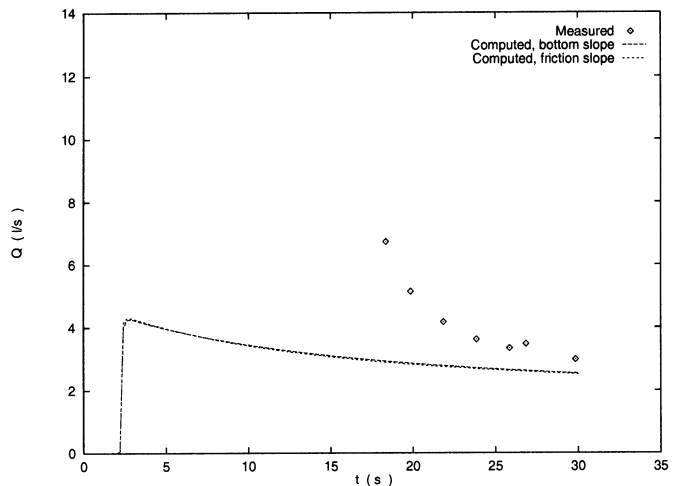


Fig. 7. Flow discharge time evolution at the end of the reach. Stony debris flow.

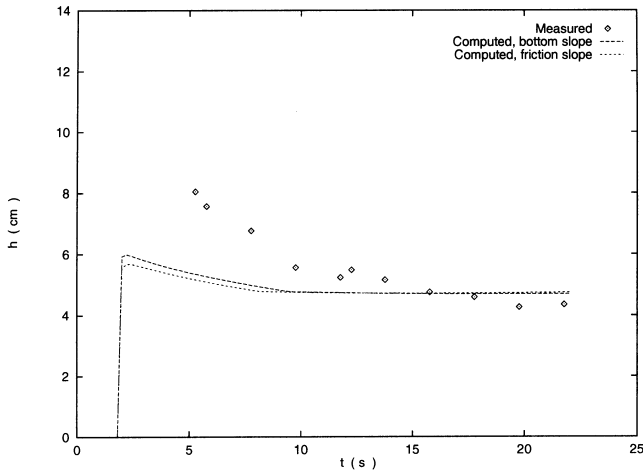


Fig. 8. Flow depth time evolution at the end of the reach. Stony to immature debris flow.

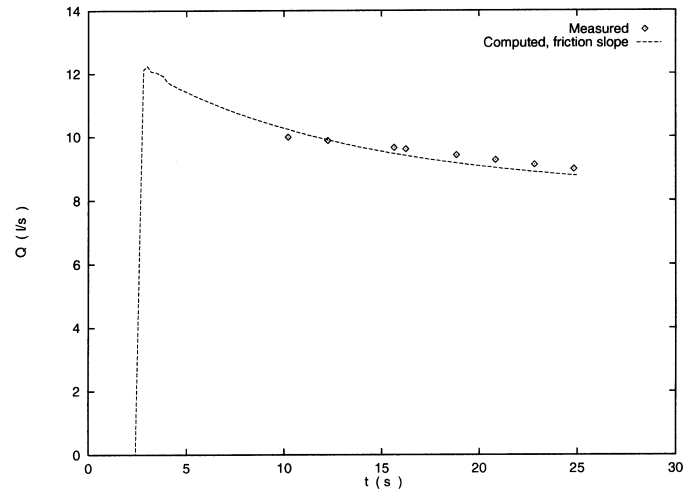


Fig. 11. Flow discharge time evolution at the end of the reach. Immature debris flow.

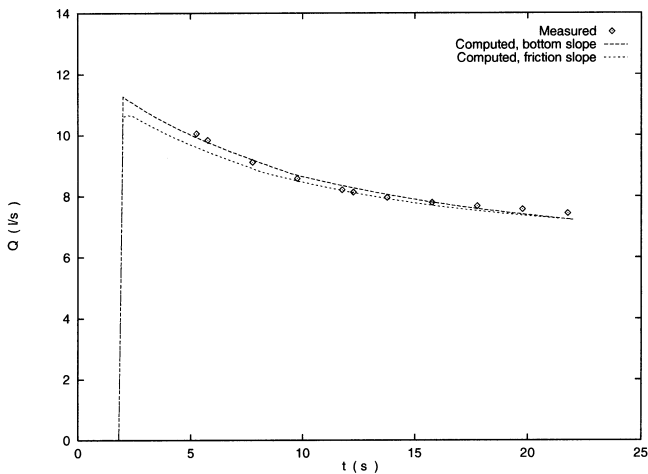


Fig. 9. Flow discharge time evolution at the end of the reach. Stony to immature debris flow.

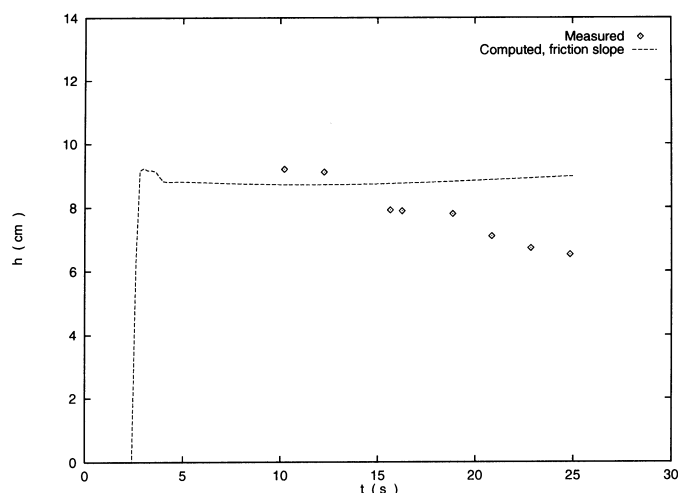


Fig. 10. Flow depth time evolution at the end of the reach. Immature debris flow.

There is a good agreement between experimental and computed values of the discharge; however the flow depth seems more problematic although the differences are most of the time less than 30%. This difference could be explained by the high uncertainty in the flow depth measurements. Experimental data (Gregoretti 1996) show that at the beginning of the process, the bottom layer of the debris flow moved much more slowly than the average flow velocity. The mathematical model does not consider this “stratification” and so the flow depth is underestimated during the first phase of the phenomenon.

5 Conclusions

A first-order upwind scheme for 1D modelling of debris flow is presented. Of practical interest is its ability to describe easily the processes involved, as it is shown in this work. A modification of the momentum balance equation was performed to permit density changes in time and space. Comparisons of the two formulations demonstrated that debris density variations are not strong enough to affect the results. This confirms the hypothesis followed by several authors, who ignore the effects of the spatial and temporal variations of density.

Dry bed initial conditions do not constitute any problem for the numerical scheme and the advance of the front is well resolved. Different channel and flow configurations of the problem have been tested varying friction, sediment density, bed slopes, parameters, etc. without difficulties. Comparisons with different space intervals, Δx , led to the same results. Mass conservation errors have been controlled during all the computations and were always found lower than 3%.

Some numerical tests and comparisons with experimental data have been carried out to validate and explore the limitations of the scheme and the models used, as the Egashira-Ashida and Takahashi models for the erosion/deposition velocity or the distinction between different types of flow and their respective friction terms.

It is worth noting that Egashira and Takahashi models for the erosion/deposition rate give similar results in the test cases presented when the empirical coefficients are properly adjusted. Strong differences arise from the fact of using the bed inclination or the friction slope in the erosion formula. The introduction of the friction slope instead of the bottom slope allows to tackle situations of erosion on counterslopes.

In future work we intend to extend the scheme to second order in both space and time in order to achieve better accuracy, and make some comparisons to determine the influence of the number of nodes and cells used in each case and the CFL constraint. Irregular geometries for the cross section with their changes in time and space will be considered. Our main objective will be the development of a 2D upwind scheme to model the propagation of debris flow on alluvial fans. Besides that, we plan to test the use of different equations of motion for the solid and liquid phases.

The results are strongly influenced by the upstream boundary conditions and the friction terms. We will study other possibilities to overcome this problem in order to have better approximations to real world events.

Finally, we think that the model proposed and the numerical algorithm presented will be a valid tool not only to simulate real world situations but also to interpret laboratory experiments.

Acknowledgements

The authors kindly acknowledge Marco Gregoretti for the documentation on his experimental data. This work was partially granted by the programme "Morfodinamica Fluviale e Costiera" of the University Ministry (MURST) and by the Italian-Spanish Integrated Action programme.

List of symbols

\mathbf{A}	Jacobian matrix
$\tilde{\mathbf{A}}$	approximated Jacobian matrix
A	debris flow cross section area
a^k	eigenvalues of the Jacobian matrix
\bar{a}^k	average values of the eigenvalues
a_B	empirical constant
b	width of the channel
CFL	Courant number
c	dimensionless sediment volumetric concentration
c_{eq}	equilibrium concentration for uniform flow
c_v	parameter related to the concentration of sediments in the bed layer
c^*	coarse fraction concentration in the static debris bed
c_D^*	volumetric sediment concentration on a static bed just after deposition
c'_{eq}	equilibrium concentration for non-uniform flow
d	mean effective diameter of the sediment particles
e^k	eigenvectors of the Jacobian matrix
\tilde{e}^k	average values of the eigenvectors
\mathbf{F}	flux vector in the x direction
\mathbf{F}^*	numerical flux

g	acceleration due to gravity
\mathbf{H}	source term
h	debris flow depth
i	bed erosion/deposition velocity
j	cell index
k	number of equations index
K	empirical coefficient
m	empirical constant
P	wetted perimeter
Q	debris flow discharge
R_h	hydraulic radius
S_0	bed slope
S_f	friction term
s	density ratio
t	time level
\mathbf{U}	vector of conservative variables
u	mean velocity in a cross section
v	celerity
\tilde{v}	average value of the celerity
x	space coordinate
z	bed level
α	dynamic internal angle of friction
α^k	coefficients of the eigenvector's decomposition
β	momentum correction coefficient
δ_d	empirical constant for deposition
δ_e	empirical constant for erosion
Δx	space interval
ε^k	entropy parameter
ϕ	static internal friction angle
λ	linear concentration
ψ^k	absolute values of the eigenvalues of $\tilde{\mathbf{A}}$
ρ	debris flow density
ρ_l	liquid density
ρ_s	sediment density
ρ^*	density of static bed
ρ_D^*	density of static bed just after deposition
θ	bed inclination
θ_e	equilibrium angle
θ_f	energy line angle

References

1. Alcrudo, F., García-Navarro P., "Flux difference splitting for 1D open channel flow equations", *Int. J. for Num. Meth. in Fluids*, Vol 14, pp. 1009-1018, 1992.
2. Armanini, A., Fraccarollo L., "Critical conditions for debris flow", *Debris Flow Hazard Mit.: Mech., Pred. and Assessment*, ASCE, 1997.
3. Bagnold, R. A., "Experiments on a gravity-free dispersion of large solid spheres in a newtonian fluid under shear", *Proc. R. Soc. London, Ser. A* 225, pp. 49-63, 1954.
4. Chen, C.L., "Generalized viscoplastic modelling of debris flow", *J. Hyd. Res.*, ASCE, 114(3), 1988.
5. Chow, V.T., "Open Channel Hydraulics", MacGraw-Hill Book Co. Inc., 1959.
6. Di Silvio, G., Gregoretti, C., "Gradually varied debris flow along a slope", *Debris Flow Hazard Mit.: Mech., Pred. and Assessment*, ASCE, 1997.

7. Egashira, S., Ashida, K., "Sediment transport in steep slope flumes", Proc. of Roc Japan Joint Seminar on Water Resources, 1987.
8. Egashira, S., Miyamoto, K., Takahiro, I., "Constitutive equations of debris flows and their applicability", Debris Flow Hazard Mit.: Mech., Pred. and Assessment, ASCE, 1997.
9. Fraccarollo, L., "Un modello matematico bidimensionale per la mappatura del rischio da colata di detriti", GNDCI, Linea 1, pp. 97-105, 1995.
10. Ghilardi, P., Natale, L., "Colate detritiche: equazioni unidimensionali per le corrente in moto vario", Internal Rep., Univ. of Pavia, 1998.
11. Gregoretto, C., "Studio sperimentale delle colate detritiche originate dall'erosione progressiva di un pendio", PhD dissertation, Univ. of Padova, 1996.
12. Harten, A., Hyman, P., Self adjusting grid methods for one dimensional hyperbolic conservation laws, J. of Comp. Phys., Vol. 50, pp. 235-269, 1983.
13. Hirano, M., Harada, T., Banihabib, M.E., Kawahara, K., "Estimation of hazard area due to debris flow", Debris Flow Hazard Mit.: Mech., Pred. and Assessment, ASCE, 1997.
14. Honda, N., Egashira, S., "Prediction of debris flow characteristics in mountain torrents", Debris Flow Hazard Mit.: Mech., Pred. and Assessment, ASCE, 1997.
15. Hutter, K.B., Svendsen, Rickenmann, D., "Debris flow modelling: a review", Continuum Mech. and Thermodyn., Vol. 8, pp. 1-35, 1996.
16. Iverson, R.M., "Hydraulic modelling of unsteady debris-flow surges with solid-fluid interaction", Debris Flow Hazards Mitigation: Mech., Pred. and Assessment, ASCE, 1997.
17. Jan, C.D., "A study on the numerical modelling of debris flow", Debris Flow Hazards Mitigation: Mech., Pred. and Assessment, ASCE, 1997.
18. Jin, M., Fread, D. L., "1D routing of mud/debris flow using NWS FLDWAV model", Debris Flow Hazard Mit.: Mech., Pred. and Assessment, ASCE, 1997.
19. Laigle, D., Coussot, P., "Numerical modelling of mudflows", J. of Hyd. Eng., 1997.
20. Mizuyama, T., Yazawa, A. "Computer simulation of debris flow depositional processes", Proc. of the Corvallis Symp., 1987.
21. Nakagawa, H., Takahashi, T., "Estimation of a debris flow hydrograph and hazard area", Debris Flow Hazards Mitigation: Mech., Pred. and Assessment, ASCE, 1997.
22. O'Brien, J.S., Julien, P.J., Fullerton W.T., "Two-dimensional water flood and mudflow simulation", J. of Hyd. Eng., Vol. 119(2), 1993.
23. Rickenmann, D., Koch, T., "Comparison of debris flow modelling approaches", Debris Flow Hazards Mitigation: Mech., Pred. and Assessment, ASCE, 1997.
24. Roe, P.L., "Approximate Riemann solvers, parameter vectors and difference schemes", J. of Comp. Phys., Vol. 43, pp. 357-372, 1981.
25. Savage, S.B., Hutter, K., "The motion of a finite mass of granular material down a rough incline", J. of Fluid Mech., Vol. 199, pp. 177-215, 1989.
26. Scotton, P., Armanini, A., "Experimental investigation of roughness effects of debris flow channels", 6th Workshop on two-phase Flow prediction, Erlangen, 1992.
27. Shieh, C.L., Jan, C. D., Tsai, Y. F., "A numerical simulation of debris flow and its application", Natural Hazard, Vol. 13, pp. 39-54, 1996.
28. Takahashi, T., Tsujimoto, H., "Delineation of the debris flow hazardous zone by a numerical simulation method", Int. Symp. on Erosion, Debris Flow and Disast. Prevent, 1985.
29. Takahashi, T., Nakagawa, H., Kuang, S., "Estimation of debris flow hydrograph on varied slope bed", Proc. of the Corvallis Symp., 1987.
30. Takahashi, T., "Debris Flow", Balkema, Rotterdam, 1991.
31. Takahashi, T., Nakagawa, H., "Flood/debris flow hydrograph due to collapse of a natural dam by overtopping", J. of Hydroscience and Hyd. Eng., 1994.
32. Toro, E.F., Riemann solvers and upwind methods for fluid dynamics, Springer-Verlag, 1996.
33. Yazawa, A., Mizuyama, T., "Measures against debris flow on roads", Techn. Memor. of Public Works Res. Inst., Ministry of Construction, Japan, Vol. 1492, 1987.